International Journal of Nanomedicine

Dovepress
Taylor & Francis Group

Open Access Full Text Article

ORIGINAL RESEARCH

# AuNRs-PPARγmAb Induce Targeted Adipocyte Apoptosis Through Photothermal Effects for Effective Localized Fat Reduction

Yiping Hu[1,*], Kui Xiao[1,*], Ziang Chen[1], Shali Ou[2], Chao Sima[3], Haiyang Wang[4], Jinli Zhang[1], Zhi Zhang[1], Xiaojian Li[1]

[1]Department of Burns and Plastic Surgery, Guangzhou Red Cross Hospital, Jinan University, Guangzhou, Guangdong, 510000, People's Republic of China; [2]Department of Oral and Maxillofacial Surgery, Women and Children's Medical Center Affiliated to Guangzhou Medical University, Guangzhou, Guangdong, 510000, People's Republic of China; [3]Department of Surgery, Shenzhen Guangming District People's Hospital, Shenzhen, Guangdong, 518107, People's Republic of China; [4]College of Life Sciences, Anhui Normal University, Wuhu, Anhui, 241000, People's Republic of China

*These authors contributed equally to this work

Correspondence: Xiaojian Li; Zhi Zhang, Department of Burns and Plastic Surgery, Guangzhou Red Cross Hospital, Jinan University, 396 Tongfu Road, Guangzhou, 510000, People's Republic of China, Email lixj64@163.com; zhangzhicc48@163.com



**Background:** Non-invasive fat reduction and body contouring technologies have rapidly advanced in plastic surgery. Although various devices have been developed globally for body sculpting, the mechanisms and long-term efficacy of non-surgical fat reduction are still debated. While gold nanorods (AuNRs) have been extensively studied in cancer treatment, their potential in fat reduction has not been explored. This study aims to design a novel nanoplatform combining AuNRs with a PPARγ monoclonal antibody (PPARγmAb) for effective photothermal fat reduction therapy.

**Methods:** AuNRs were chemically activated by adding 1-ethyl-3-(3-dimethylaminopropyl) carbodiimide (EDC) activator, followed by the addition of PPARγmAb for reaction. Simultaneously, adipose-derived stem cells were induced to differentiate into adipocytes, and an obese mouse model was established. Differentiated adipocytes and obese mice were treated with AuNRs-PPARγmAb and exposed to 808nm near-infrared (NIR) laser irradiation to evaluate fat reduction effects and biocompatibility.

**Results:** The PPARγmAb modification did not significantly affect the optical properties of AuNRs but greatly increased their retention in adipocytes. Compared to AuNRs alone, AuNRs-PPARγmAb showed a stronger photothermal effect on adipocytes under 808 nm near-infrared laser irradiation, inducing cell apoptosis. In obese mice, AuNRs-PPARγmAb treatment significantly reduced adipose tissue weight, size, and thickness, with no major histopathological damage observed in organs. Hematological parameters, as well as liver and kidney function, remained unchanged, confirming the biocompatibility and fat-reducing efficacy of the treatment.

**Conclusion:** AuNRs-PPARγmAb, when exposed to 808nm NIR laser irradiation, effectively targets and induces apoptosis in adipocytes, leading to significant fat reduction. This targeted approach offers a promising method for non-surgical, localized fat reduction. Compared to other fat reduction treatments, it provides the advantages of high specificity, minimal invasiveness, and fewer side effects, highlighting its potential for clinical application.

**Keywords:** obesity, non-surgical fat reduction, gold nanorods, PPARγ, photothermal therapy

## Introduction

Obesity is a major global health challenge characterized by abnormal or excessive fat accumulation, which increases the incidence and mortality risk of various diseases.[1,2] Specifically, increased fat distribution in the waist and hip areas is closely associated with heart disease and diabetes.[3,4] Currently, methods for treating obesity include dietary control, pharmacotherapy, and surgical intervention.[5] However, as aesthetic demands increase, people not only seek to maintain health, but their desire for a good physique and perfect body shaping is also growing.

Received: 19 February 2025
Accepted: 23 June 2025
Published: 2 August 2025

Common methods for reducing subcutaneous abdominal fat include surgical and non-surgical treatments.[6,7] Liposuction, as an outpatient procedure, sculpts the body by removing subcutaneous fat,[8,9] while abdominoplasty reshapes the abdomen by excising loose skin and excess fat.[10] However, these surgical methods have significant drawbacks, including trauma, pain, and prolonged recovery periods,[11,12] emphasizing the need for non-surgical treatments that are better suited for localized obesity. Lipolysis techniques, which are currently common non-surgical methods, work by reducing localized fat through the disruption of adipocyte membranes.[13] These techniques encompass various methods, such as pharmacological, ultrasound, thermal injury, and laser treatments.[14,15] However, these methods currently lack specificity, potentially damaging surrounding non-fat tissues and increasing the risk of side effects. The pursuit of non-invasive, highly comfortable, and effective fat reduction and body contouring treatments has become a prominent research focus in modern plastic surgery.

In recent years, nanotechnology has seen widespread application in biomedical research.[16,17] In the research on using nanomaterials for obesity treatment, multiple teams have achieved notable outcomes. The "nano - sandwich" structure (P3 - HA/PM@BP) developed by the Xiao team enhances the M2/M1 ratio in adipose tissue, improving the metabolic indicators and insulin sensitivity of obese mice and establishing a novel metabolic - regulation - based anti - obesity model.[18] Simultaneously, the Su team's macrophage - membrane - camouflaged and P3 - peptide - modified rHDL nanocarrier, which can co - load rosiglitazone and sildenafil, shows a "self - enhancing" synergistic effect in mouse models, enriching treatment methods and providing a new direction for adipose - targeted therapy.[19] The Choi team innovatively developed an SA - OP platform using hyaluronic acid microneedles for gene therapy, enabling efficient shRNA delivery to adipocytes and creating a new approach for treating obesity and related metabolic syndromes.[20] These teams' efforts have advanced nanotechnology in obesity treatment from diverse perspectives. However, in the context of non-surgical fat reduction, although AuNRs can also utilize the photothermal effect to act on fat cells and achieve fat reduction, they are not specifically targeted at fat cells. Therefore, inducing the apoptosis of adipocytes through the photothermal effect of AuNRs and developing an AuNRs system with the ability to specifically recognize adipocytes will be the key breakthrough point for achieving precise fat reduction.

Peroxisome proliferator-activated receptor gamma (PPARγ) is a nuclear receptor that plays a crucial role in lipid, glucose, and amino acid metabolism.[21] PPARγ is essential for the survival of fat cells, and its deletion in mature adipocytes leads to cell death.[22] Although PPARγ is expressed in various cell types, particularly in metabolism-related cells, it is highly expressed in adipocytes and serves as a critical regulator of adipocyte differentiation and function.[23] Although PPARγ is mainly located in the nucleus and exerts transcriptional regulatory functions, at the stage when it is synthesized in ribosomes and has not yet entered the nucleus, PPARγmAb can, with its high specificity, accurately recognize and bind to intracellular PPARγ. After AuNRs are modified with PPARγ, based on the principle of specific antigen - antibody binding, the number of AuNRs in adipocytes increases significantly, and their retention time is notably prolonged. AuNRs enter adipocytes and gradually approach the nucleus through intracellular endocytic transport. During this process, AuNRs, by virtue of their unique photothermal effect, cause a local temperature increase in adipocytes, thereby promoting the apoptosis of adipocytes.

In summary, this study proposes a new non-surgical fat reduction hypothesis: localized adipose tissue reduction by conjugating PPARγmAb with AuNRs, exploiting their relevant specific binding in adipocytes and selectively destroying adipocytes under 808nm NIR laser irradiation using the photothermal effect of AuNRs. This method is expected to provide a safe and efficient new approach for localized fat reduction (Figure 1).

# Methods and Materials

## Synthesis of AuNRs-PPARγmAb

To prepare AuNRs-PPARγmAb and AuNRs-PPARγmAb-FITC, we initially acquired AuNRs from Biotyscience and characterized them. We then sonicated the AuNRs to ensure a uniform distribution and chemically activated them using 1-ethyl-3-(3-dimethylaminopropyl) carbodiimide (Servicebio, China). Following this, we passed PPARγmAb (Affinity, USA) through a G25 centrifugal column to remove salts and then added it to the activated AuNRs solution, allowing the reaction to proceed at room temperature to form the AuNRs-PPARγmAb complex.

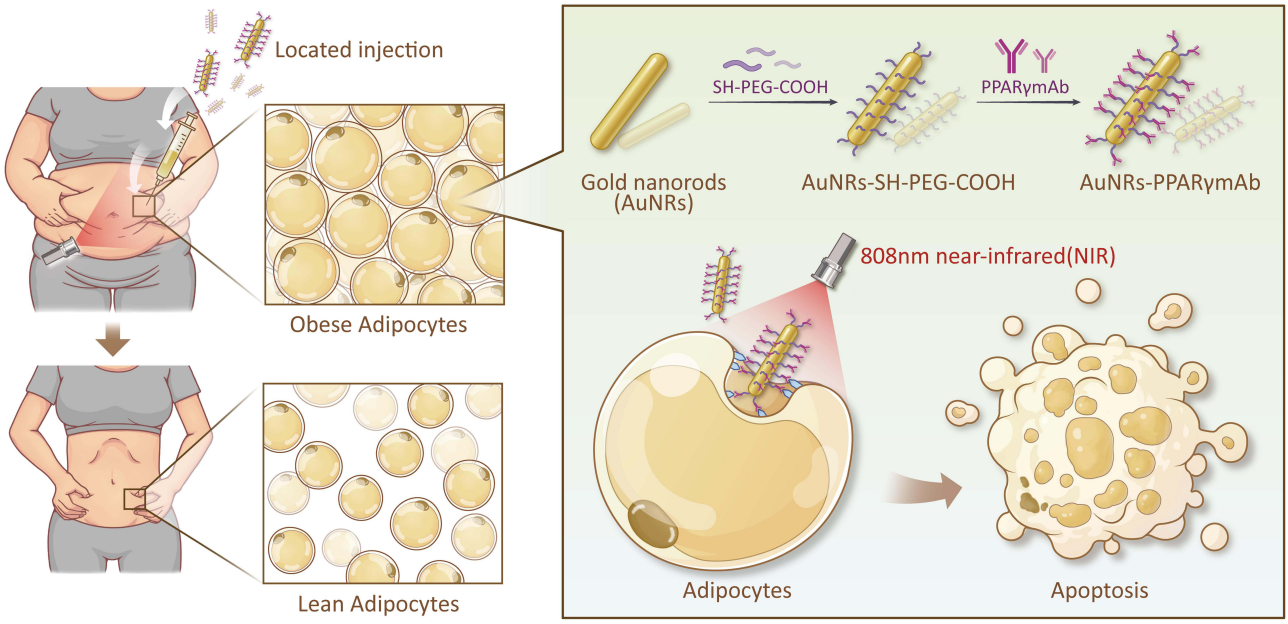


**Figure 1** Fat Reduction Treatment Strategy via Photothermal Effect of AuNRs-PPARγmAb. This figure illustrates an innovative local fat reduction treatment strategy: by injecting AuNRs-PPARγmAb into adipose tissue, followed by laser irradiation to activate the photothermal effect of the AuNRs, which specifically induces apoptosis of adipocytes, thereby significantly reducing the number of fat cells and ultimately achieving fat reduction.

We purified and stabilized the solution by centrifugation and resuspension in PBS (Corning, China), storing the final product at 4°C. To obtain AuNRs-PPARγmAb-FITC, we incorporated FITC (Thermo Fisher Scientific, USA) into the AuNRs-PPARγmAb complex. Throughout the process, we also utilized UV-vis spectroscopy to observe the optical absorption characteristics of AuNRs-PPARγmAb and AuNRs at a wavelength of 808nm.

## Isolation and Culture of Human Adipose-Derived Stem Cells (hADSCs)

All patients provided informed consent, and adipose tissue samples were collected, processed, and analyzed under the guidance of the Ethics Committee of Guangzhou Red Cross Hospital (Ethics Approval No: 2023-222-01). Surgically discarded adipose tissue, with informed consent, was processed in a sterile laminar flow hood. Impurities were removed, and the tissue was washed three times with PBS containing penicillin and streptomycin. The tissues were cut into small pieces and digested with 0.2% type I collagenase (Sigma, USA) for 60 minute. The cells were then centrifuged to collect the cell pellet, which was resuspended in PBS and centrifuged again. Finally, the cells were resuspended in DMEM/F12 (Corning, China) medium containing 10% FBS (Gibco, Australia). The cells were seeded in culture dishes and cultured at 37°C in an environment of 95% air and 5% $CO_2$, with regular medium changes. Cells were passaged when confluence exceeded 80%, and cells from passages 3–5 were used for subsequent experiments.

## Adipogenic Induction of hADSCs

Human adipose-derived stem cells (hADSCs) in the logarithmic growth phase were seeded at an appropriate density in DMEM/F12 and hADSCs medium and cultured at 37°C with 5% $CO_2$, maintaining cell density at 60–80% confluence. Once the cells reached confluence, the supernatant was discarded, and adipogenic induction medium A (containing dexamethasone (Beyotime, China), indomethacin (Beyotime, China), 3-isobutyl-1-methylxanthine (Beyotime, China), insulin (Beyotime, China), and high-glucose DMEM) was added to induce differentiation. After approximately 14 days, lipid droplets formed, and the medium was switched to adipogenic induction medium B (containing insulin and high-glucose DMEM) to stabilize adipocytes.

## Nile Red Staining

Induced adipocytes were washed with PBS 2–3 times and fixed with 4% paraformaldehyde (Servicebio, China) at room temperature for 10–15 minutes. After fixation, the cells were washed again with PBS. A staining solution of 1 μg/mL


https://doi.org/10.2147/IJN.S520656

Nile Red (Sigma, USA) was added, and the cells were incubated at room temperature in the dark for 10–15 minutes to stain the lipid droplets. After staining, the samples were washed three times with PBS, for 5 minutes each time. Finally, the samples were mounted with anti-fading mounting medium and observed under a microscope (Nikon, Japan) at an excitation wavelength of 488 nm to visualize and record the orange-red fluorescence of the lipid droplets.

## Cell Viability

In the 96-well plate that has been treated, we add 10μL of CCK-8 reagent (Beyotime, China) to each well, and then we place the plate back into the incubator to continue culturing for 1–2 hours. After the culture is finished, we use a microplate reader to measure the absorbance (OD value) of each well at a wavelength of 450nm. By comparing the OD values of treatment groups with those of the blank control group, the impact of the treatment on adipocyte activity can be calculated.

## Adipocyte Uptake of AuNRs and AuNRs-PPARγmAb

The cells were then incubated at 37°C with 5% $CO_2$ for 24 hours. Following incubation, the cells were washed 2–3 times with PBS to remove any uninternalized AuNRs or AuNRs-PPARγmAb. Subsequently, the cells were fixed with 2.5% glutaraldehyde (Sigma, USA) for 30 minutes. The fixed cell samples were then dehydrated, embedded, and ultrathin sections were prepared for observation under a transmission electron microscope (TEM) to analyze the uptake of AuNRs and AuNRs-PPARγmAb by the adipocytes.

## Immunofluorescence Staining

The culture medium was removed, and the cells were fixed with 4% paraformaldehyde for 30 minutes. The samples were then treated with 0.3% Triton X-100 (Beyotime, China) for 10 minutes and blocked with 5% goat serum (Beyotime, China) for 1 hour. The samples were incubated with primary antibodies overnight at 4°C: rabbit anti-Caspase-3 (1:100, Zenbio, China). Subsequently, secondary antibodies (1:100; Zenbio, China) were added, and the cells were stained with DAPI (Beyotime, China) for 5 minutes to label the nuclei. The stained sections were imaged using a microscope.

## Flow Cytometry Analysis

After treatment, the cells are washed with PBS, then trypsinized with 0.25% trypsin without EDTA to detach them, and resuspended in binding buffer. The cells are stained with Annexin V- FITC (Sigma, USA) and PI (Beyotime, China), incubated in the dark at room temperature for 10–15 minutes, followed by the addition of binding buffer and kept on ice for flow cytometry analysis. The flow cytometer is equipped with detection channels for Annexin V- FITC and PI, gated based on forward scatter (FSC) and side scatter (SSC), and collects and analyzes data from at least 10,000 cells using software to determine the apoptosis rate.

## Western Blotting

Cells were collected and lysed with RIPA lysis buffer (Beyotime, China) containing protease and phosphatase inhibitors (Sigma, USA). The lysates were centrifuged at 12,000 rpm for 30 minutes at 4°C, and the supernatant was collected. Proteins were separated by SDS-PAGE and transferred to 0.45 μm PVDF membranes (Millipore, USA). The membranes were blocked with QuickBlock™ blocking buffer (Beyotime, China) and incubated with primary antibodies overnight at 4°C. The primary antibody used was rabbit anti-Bax (1:100, Zenbio, China). Subsequently, the membranes were incubated with secondary antibodies (Zenbio, China) for 2 hours at room temperature. Protein detection was performed using an enhanced chemiluminescence kit (Thermo Fisher Scientific, USA), and protein quantification was carried out using ImageJ software.

## Establishment of Obese Mice Model

Four-week-old C57BL/6 mice were purchased from the Guangzhou Ruige Biotechnology Center. The animal experiments were approved by the Guangzhou Red Cross Hospital (Approval No. 2024-078-01). The mice were initially fed a standard diet for two weeks before gradually transitioning to a high-fat diet. Specifically, the mice were first given a diet

consisting of 20% standard diet and 80% high-fat diet (containing 60 kcal% fat). The proportion of high-fat diet was gradually increased each week, reaching a full 60 kcal% fat diet by the 7th week. After approximately 10 weeks, the mice developed obesity, defined as a body weight of around 42g. The mice were then randomly divided into four groups, with five mice per group.

## In vivo Efficacy Testing

Upon reaching the required body weight, mice were randomly divided into four groups: Control, NIR, AuNRs+NIR, and AuNRs-PPARγmAb+NIR. After shaving the left inguinal area of all mice, the following treatments were administered:

- Control: Injected with 0.3 mL of PBS into the left inguinal fat pad.
- NIR group: Exposed to NIR light, no injection.
- AuNRs+NIR group: Injected with 0.3 mL of 0.1 mg/mL AuNRs solution into the left inguinal fat pad, then exposed to NIR light.
- AuNRs-PPARγmAb+NIR group: The mice were injected with 0.3 mL of 0.1 mg/mL AuNRs-PPARγmAb into the left inguinal fat pad. They were then exposed to NIR light.

One hour after injection, the NIR, AuNRs+NIR, and AuNRs-PPARγmAb+NIR groups were exposed to an 808 nm NIR laser with a power density of 0.7 W/cm² for 5 minutes on the left inguinal area. This irradiation was performed once daily for three days, including the day of injection. Immediately after each irradiation, thermal imaging was used to capture and record the surface temperature of the left inguinal area of the mice. After three consecutive days of irradiation, the thickness of the fat pad tissue in the left and right inguinal areas was observed and recorded using an ultrasound machine. Starting from the first day of irradiation, all mice continued to receive a high-fat diet, and body weight was recorded every two days. At the end of the experiment (14 days), the mice in each group were euthanized, and the bilateral fat pad tissues were dissected, weighed, photographed, and analyzed to evaluate the difference in fat pad weight and its proportion of total body weight.

## Masson and Eosin Staining

First, the adipose tissue was embedded in paraffin and sectioned into 4-micron-thick slices, which were then hydrated using ethanol of different concentrations. For Eosin staining, the washed sections were stained with hematoxylin for about 5 minutes and then with eosin for 5 minutes. After staining, the sections were dehydrated, mounted, and observed and photographed under a microscope. For Masson staining, formalin-fixed paraffin-embedded adipose tissue sections were stained with hematoxylin for 8 minutes, followed by differentiation with 1% hydrochloric acid ethanol for 15 seconds, staining with Masson's blue solution for 15 seconds, and then with acid fuchsin for 5 minutes. The sections were washed with 1% phosphomolybdic acid solution for 2 minutes, then stained with aniline blue for 2 minutes. The sections were dehydrated three times with absolute ethanol for 10 seconds each, followed by three treatments with xylene for 1 minute each. Finally, the sections were mounted with neutral resin and observed under a microscope.

## TUNEL Staining

First, cells are washed with PBS, then fixed with 4% paraformaldehyde for 30 minutes. After fixation, they are washed again with PBS, followed by pre-treatment with PBS containing Triton X-100 to enhance cell membrane permeability. Concurrently, fixed adipose tissue sections are deparaffinized and rehydrated, and treated with proteinase K to further increase cell membrane permeability. Next, the TUNEL detection solution (Beyotime, China) is prepared by mixing TdT enzyme and TUNEL fluorescence labeling solution in a 1:10 ratio. The TUNEL detection solution is added to the samples and incubated at 37°C in the dark for 60 minutes. After staining, the sections are mounted with an anti-fade mounting medium. Finally, the stained sections are observed under a fluorescence microscope to identify and count apoptotic cells.

## In vivo Safety Evaluation

On day 14 following treatment, blood biochemical parameters were assessed in mice from each group, including liver enzymes such as alanine aminotransferase (ALT) and aspartate aminotransferase (AST), lipid profiles comprising total cholesterol (TC) and triglycerides (TG), renal function evaluated through creatinine levels (CREA), and urea levels. Moreover, post-mortem collection of liver, kidney, and spleen tissues was conducted for pathological examination to evaluate safety indicators.

## Statistical Analysis

Quantitative results were expressed as mean ± standard deviation (s.d.) and depicted with error bars in all figures. Statistical analysis was performed using GraphPad Prism 7. Data were analyzed using one-way ANOVA or two-way ANOVA. A P-value of less than 0.05 was considered statistically significant (*$P < 0.05$, **$P < 0.01$, ***$P < 0.001$).

# Results

## Characterization of AuNRs-PPARγmAb and Adipogenic Induction and Uptake by Adipose-Derived Stem Cells

The transmission electron microscopy (TEM) showed at the AuNRs have dimensions of 32±2 nm in diameter and 115±5 nm in length, with an aspect ratio of 3.6, as shown in Figure 2A. Additionally, UV-vis spectroscopy showed that the absorption peak of AuNRs-PPARγmAb at 808nm remains unchanged (Figure 2B). Concurrently, to verify the adipogenic differentiation capability of adipose-derived stem cells, we successfully induced adipocytes through 14 days of adipogenic induction, as shown in Figure 2C. This confirmed successful differentiation for subsequent experiments. We were surprised to find that the AuNRs conjugated with PPARγmAb specifically entered adipocytes, while not entering endothelial cells or fibroblasts, highlighting their cellular selectivity, as shown by the fluorescence imaging in Figure 2D. Subsequently, TEM observations (Figure 2E and F) further confirmed that conjugation with PPARγmAb significantly enhanced the remains of AuNRs in adipocytes. In summary, these results further confirm that the conjugation of AuNRs with PPARγmAb significantly enhances the uptake efficiency of AuNRs by adipocytes after successful induction.

## Effects of AuNRs-PPARγmAb on Adipocyte Viability and Determination of Optimal Experimental Conditions

In our initial investigation, we assessed the effects of AuNRs and AuNRs-PPARγmAb on adipocyte viability. The CCK8 cytotoxicity assay results indicated that at a concentration of 0.2 mg/mL of AuNRs, the viability of adipocytes was significantly reduced, as shown in Figure 3A. Based on this finding, we decided to use a concentration of 0.1 mg/mL for both AuNRs and AuNRs-PPARγmAb in subsequent experiments. The flowchart detailing our cellular experimental procedures is presented in Figure 3B. Subsequently, we established the optimal irradiation time, power, and concentration parameters for AuNRs-PPARγmAb in this experiment, while also monitoring cell viability after irradiation. In terms of timing, we exposed the cell solution to an 808nm laser at various power levels and observed that there was no significant temperature increase after 5 minutes (Figure 3C). Consequently, we selected 5 minutes as the duration for subsequent laser irradiation. Regarding the selection of laser irradiation power, we observed that at 0.7W/cm$^2$, the temperature was maintained around 40°C. However, when the power was increased to 0.8W/cm$^2$, the temperature exceeded 45°C, as shown in Figure 3D. Previous studies have shown that temperatures above 43°C typically cause cell necrosis.[24] Therefore, to prevent excessive temperatures from causing necrosis rather than apoptosis, we decided to use a power of 0.7 W/cm$^2$ in our subsequent experiments. To select the optimal concentration of AuNRs-PPARγmAb solution, we tested different concentrations (0, 0.05, 0.1, 0.2 mg/mL) of AuNRs-PPARγmAb and irradiated them at 0.7 W/cm² for 5 minutes. As shown in Figure 3E, there was no significant statistical difference in temperature change between the 0.1 mg/mL and 0.2 mg/mL concentrations. Moreover, as previously mentioned, the 0.2 mg/mL concentration exhibited cytotoxicity. Therefore, we chose 0.1mg/mL as the concentration for subsequent experiments. After determining the optimal time, power, and concentration parameters, we found that AuNRs-PPARγmAb significantly reduced the viability of adipocytes (Figure 3F).

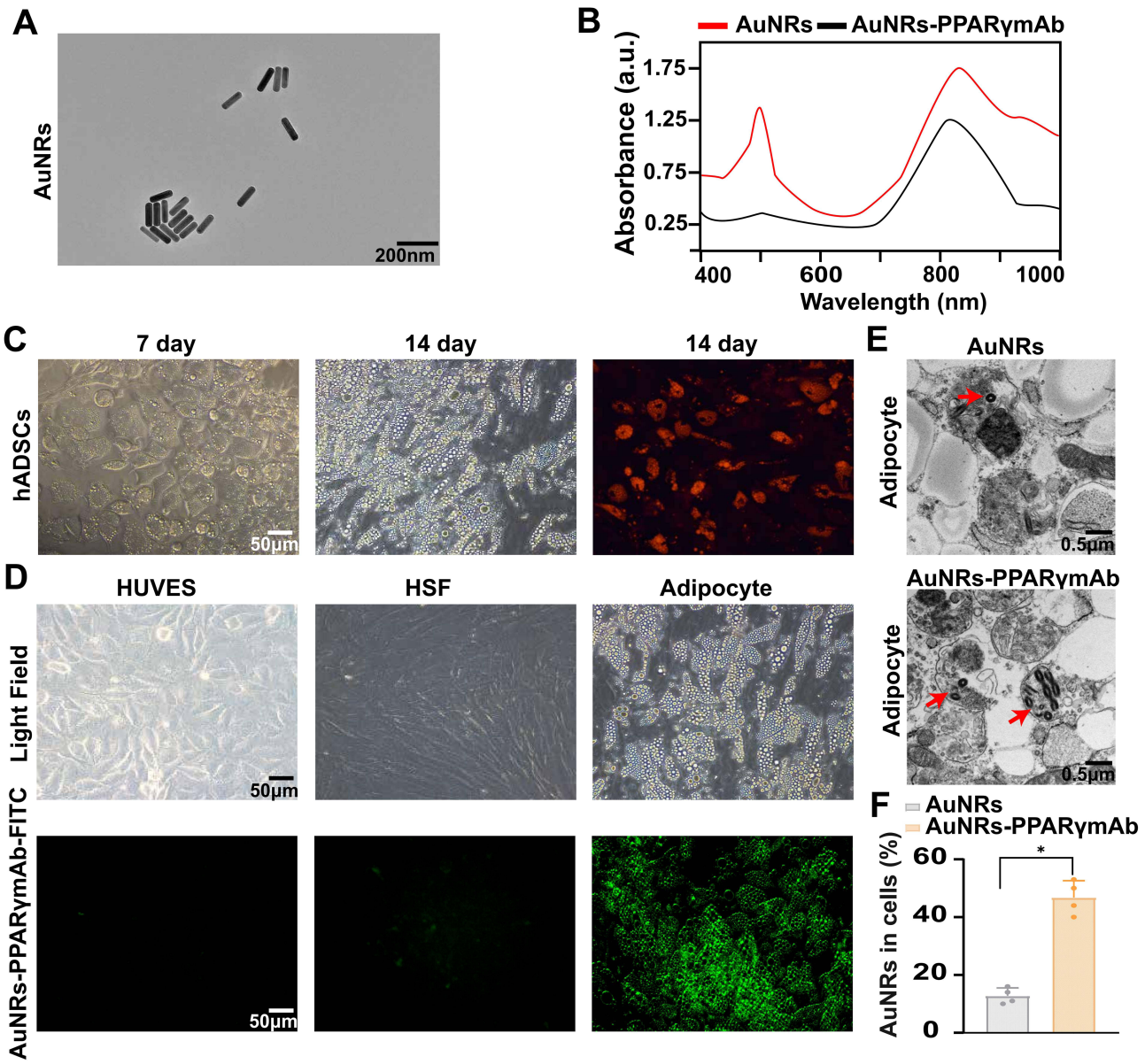


**Figure 2** AuNRs Conjugated with PPARγmAb for Targeted Uptake in Adipocytes. (**A**) The transmission electron microscopy (TEM) image displaying the dimensions of AuNRs. (**B**) UV–vis spectrum of AuNRs and AuNRs-PPARγ. (**C**) The phase contrast microscopy (PCM) image depicts the process of adipose-derived stem cells differentiating into adipocytes. (**D**) The fluorescence microscopy (FM) image showed the uptake of AuNRs-PPARγ-FITC by endothelial cells, fibroblasts, and adipocytes. (**E**) TEM image illustrates the intracellular localization of both AuNRs and AuNRs-PPARγmAb in adipocytes, with the AuNRs specifically indicated by the red arrows. (**F**) Statistical analysis of AuNRs content within adipocytes in the AuNRs and AuNRs-PPARγmAb groups. (*P < 0.05).

Ultimately, we determined that the optimal conditions for subsequent experiments were 0.1 mg/mL of AuNRs-PPARγmAb and an irradiation power of 0.7 W/cm$^2$ for 5 minutes.

## Promotion of Adipocyte Apoptosis by AuNRs-PPARγmAb

To further evaluate the reasons behind the decrease in adipocyte viability caused by AuNRs-PPARγmAb, we first analyzed adipocyte apoptosis using flow cytometry. As shown in Figure 4A, AuNRs-PPARγmAb significantly enhanced adipocyte apoptosis, with a more pronounced effect compared to AuNRs alone. In Figure 4B and C, the Western blot analysis showed that the expression of Bax protein in the AuNRs-PPARγmAb group was significantly higher than that in the control, NIR, and AuNRs groups. This suggests that AuNRs-PPARγmAb may promote cell apoptosis by upregulating the pro-apoptotic protein Bax. In Figure 4D–F, the number of caspase-positive and TUNEL-positive cells in the AuNRs-PPARγmAb group was


https://doi.org/10.2147/IJN.S520656

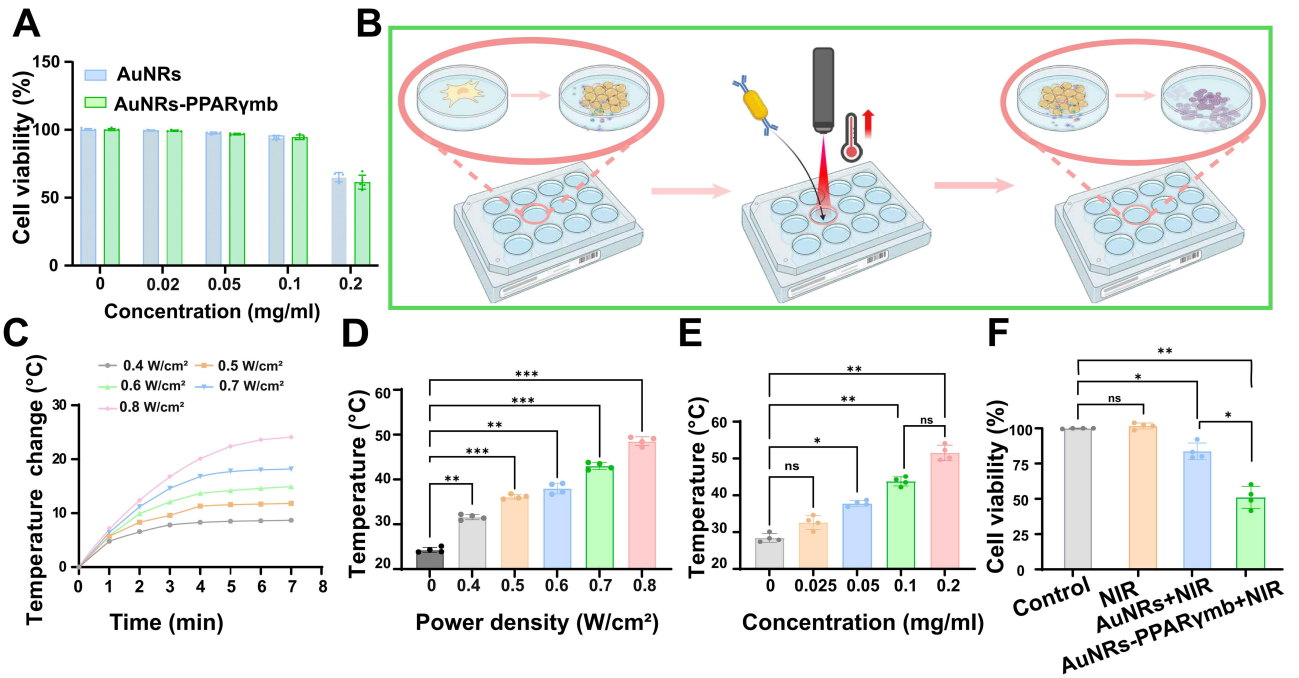


**Figure 3** Effects of AuNRs-PPARγmAb on Adipocyte Viability and Determination of Optimal Experimental Conditions. (**A**) Cytotoxicity assay results of AuNRs and AuNRs-PPARγ at different concentrations. (**B**) Flowchart outlining the experimental procedures for in vitro studies. (**C**) Temperature trends over time in cell solutions exposed to lasers at different power levels. (**D**) The temperature changes in cellular solutions after being exposed to different laser power levels for 5 minutes. (**E**) The temperature changes in cellular solutions of varying concentrations after being exposed to a 0.7 W/cm$^2$ laser power for 5 minutes. (**F**) After 5 minutes of exposure to a 0.7W/cm$^2$ laser power, the changes in cell viability among Control, NIR, AuNRs+NIR, and AuNRs-PPARγmAb+NIRgroups. (ns, no significance, *P < 0.05, **P < 0.01, ***P < 0.001).

significantly higher than those in the control, NIR, and AuNRs groups. These results further support the conclusion that AuNRs-PPARγmAb significantly promotes adipocyte apoptosis. In conclusion, these findings indicate that under photothermal conditions, AuNRs-PPARγmAb significantly promotes adipocyte apoptosis by upregulating Bax protein and increasing the number of caspase-positive and TUNEL-positive cells, outperforming the other control group.

## The Photothermal Effect of AuNRs-PPARγmAb Induced by Laser Irradiation and Its Impact on the Body Weight of Obese Mice

To evaluate the in vivo effects of AuNRs-PPARγmAb, we followed the experimental workflow illustrated in Figure 5A. Firstly, we observed that the temperature in the AuNRs-PPARγmAb group was significantly higher compared to the control, NIR, and AuNRs groups (Figure 5B). Statistical analysis presented in Figure 5C further confirms the significance of the temperature difference. Additionally, the body weight of the AuNRs-PPARγmAb group was significantly reduced compared to the control group, and this difference also reached statistical significance (Figure 5D and E). These results indicate that following NIR irradiation, the temperature increase was most pronounced in the AuNRs-PPARγmAb group, accompanied by a significant reduction in body weight.

## AuNRs-PPARγmAb Reduces the Weight, Size, and Thickness of the Left Inguinal Fat and Induces Cell Apoptosis in Obese Mice Upon Laser Irradiation

After two weeks of observation, we observed that both the area and weight of the left inguinal fat pad decreased, and the specific details are shown in Figure 6A and B. Additionally, after comparing the ratios of the area and weight between the left inguinal fat pad (LIFP) and the bilateral inguinal fat pads (BIFP), we found that there were differences between the AuNRs - PPARγmAb group and each of the other groups. As shown in Figure 6C and D, these differences were statistically significant, and the specific quantitative indicators can be found in Tables S1 and S2. The results of B-ultrasound measurement also showed that, compared with the AuNRs group, the left inguinal fat thickness in the

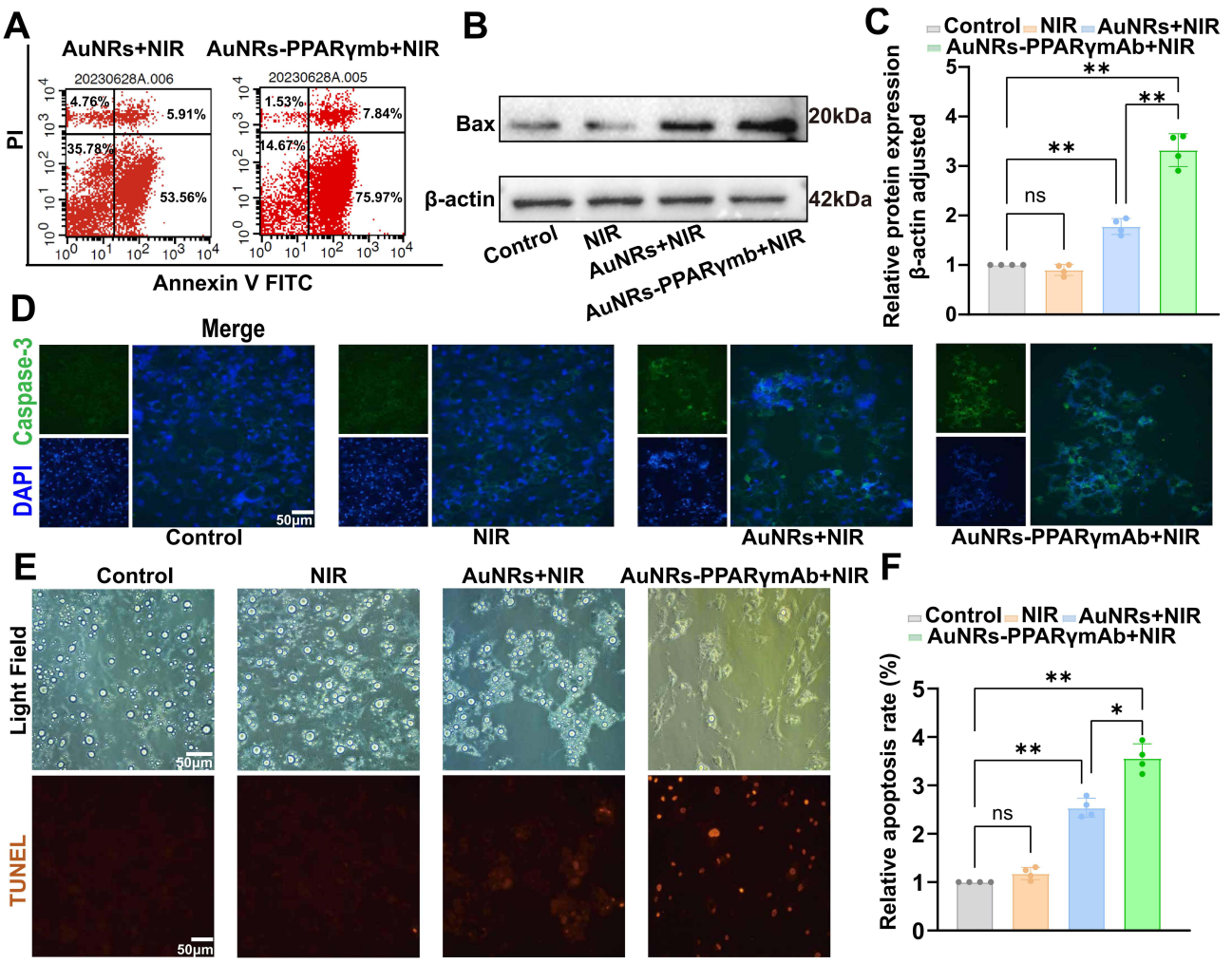


**Figure 4** Promotion of Adipocyte Apoptosis by AuNRs-PPARγmAb. (**A**) Flow cytometry analysis shows the results of adipocyte apoptosis in the AuNRs and AuNRs-PPARγmAb groups. (**B**) Western blotting assay for the detection of Bax protein in the Control, NIR, AuNRs+NIR, and AuNRs-PPARγmAb+NIR groups. (**C**) Relative Bax protein levels. (**D**) FM detects caspase-3-positive cells in the Control, NIR, AuNRs+NIR, and AuNRs-PPARγmAb+NIR groups. (**E**) FM detects TUNEL-positive cells in the Control, NIR, AuNRs+NIR, and AuNRs-PPARγmAb+NIR groups. (**F**) Quantitative analysis of TUNEL-positive cells. (ns, no significance, *P < 0.05, **P < 0.01).

AuNRs-PPARγmAb treatment group decreased, as can be seen in Figure 6E. Histological analysis further indicated that, compared with the NIR group and the AuNRs group, AuNRs-PPARγmAb would trigger mild local inflammatory responses, accompanied by the infiltration of inflammatory cells. At the same time, the number of TUNEL-positive cells in the right region of the AuNRs-PPARγmAb group increased, indicating that the number of apoptotic cells increased, as shown in Figure 6F. Combining all these results, we conclude that under near-infrared laser irradiation, AuNRs-PPARγmAb can significantly reduce the weight, size, and thickness of the inguinal fat pads in obese mice and induce apoptosis in adipose tissue.

## In vivo Biocompatibility

To assess biocompatibility, mice were euthanized 14 days after photothermal therapy. HE staining of major organs, including the liver, spleen, and kidneys, showed no significant tissue damage compared to the control group, as shown in Figure 7A. Furthermore, there were no significant differences in liver enzymes (ALT, AST), lipid profiles (TG, TC), renal function (CREA), and urea levels between the groups, as depicted in Figure 7B–G. These findings indicate that photothermal therapy using AuNRs-PPARγmAb is safe and feasible for fat reduction applications.


https://doi.org/10.2147/IJN.S520656

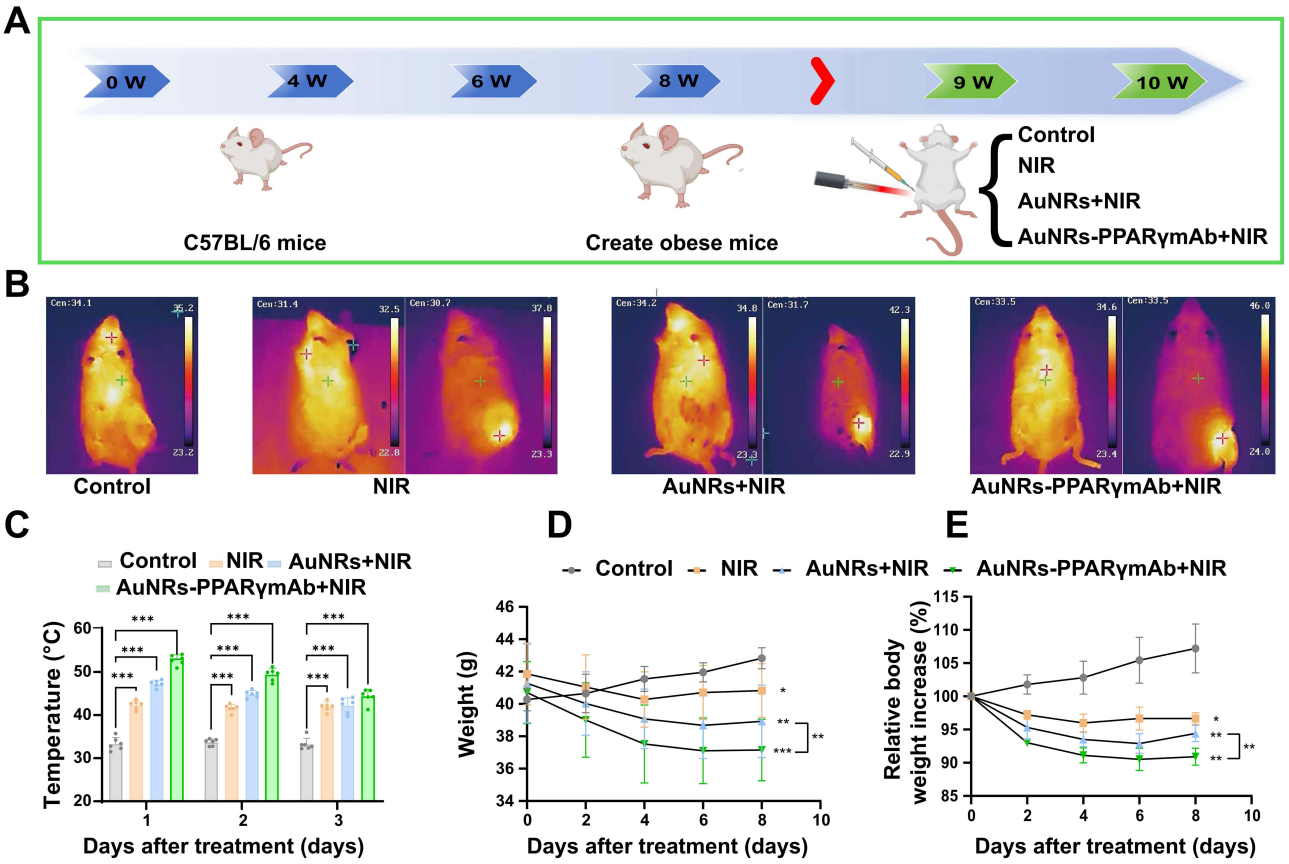


**Figure 5** Photothermal Effect and Weight Change in Obese Mice. (**A**) Flowchart outlining the experimental procedures for in vivo studies. (**B**) Temperature measurements in the Control, NIR, AuNRs+NIR, and AuNRs-PPARγmAb+NIR groups. (**C**) Statistical analysis of temperature. (**D**) Statistical analysis of weight changes over a 14-day period. (**E**) Statistical analysis of relative body weight increase over a 14-day period. (ns, no significance, *P < 0.05, **P < 0.01, ***P < 0.001).

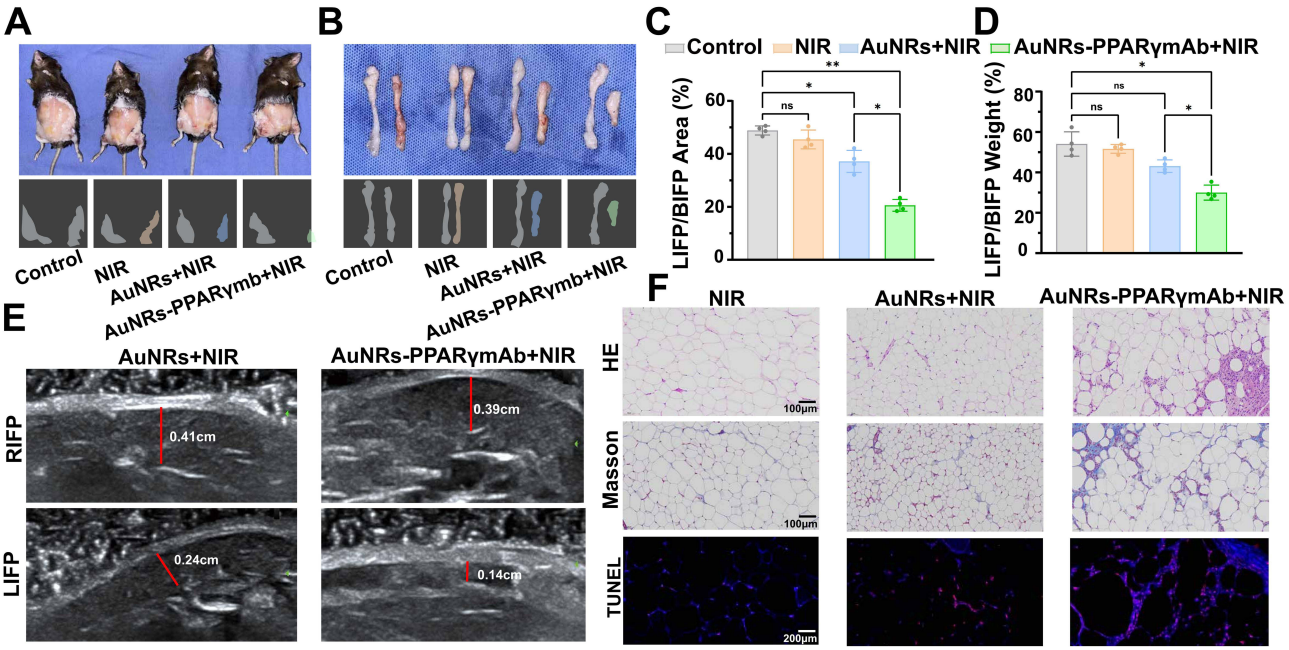


**Figure 6** AuNRs-PPARγmAb Reduces Fat and Induces Apoptosis in Obese Mice. (**A** and **B**) Visual representation of the fat pads in the left and right inguinal regions of mice. (**C**) Statistical analysis of the left inguinal fat pad (LIFP) and bilateral inguinal fat pad (BIFP) areas. (**D**) Statistical analysis of the weight of the LIFP and BIFP. (**E**) Ultrasound imaging of the thickness of the LIFP and right inguinal fat pad (RIFP) in the AuNRs and AuNRs-PPARγmAb groups. (**F**) HE, Masson, and TUNEL staining of inguinal fat in the NIR, AuNRs+NIR, and AuNRs-PPARγmAb+NIR groups. (ns, no significance, *P < 0.05, **P < 0.01).

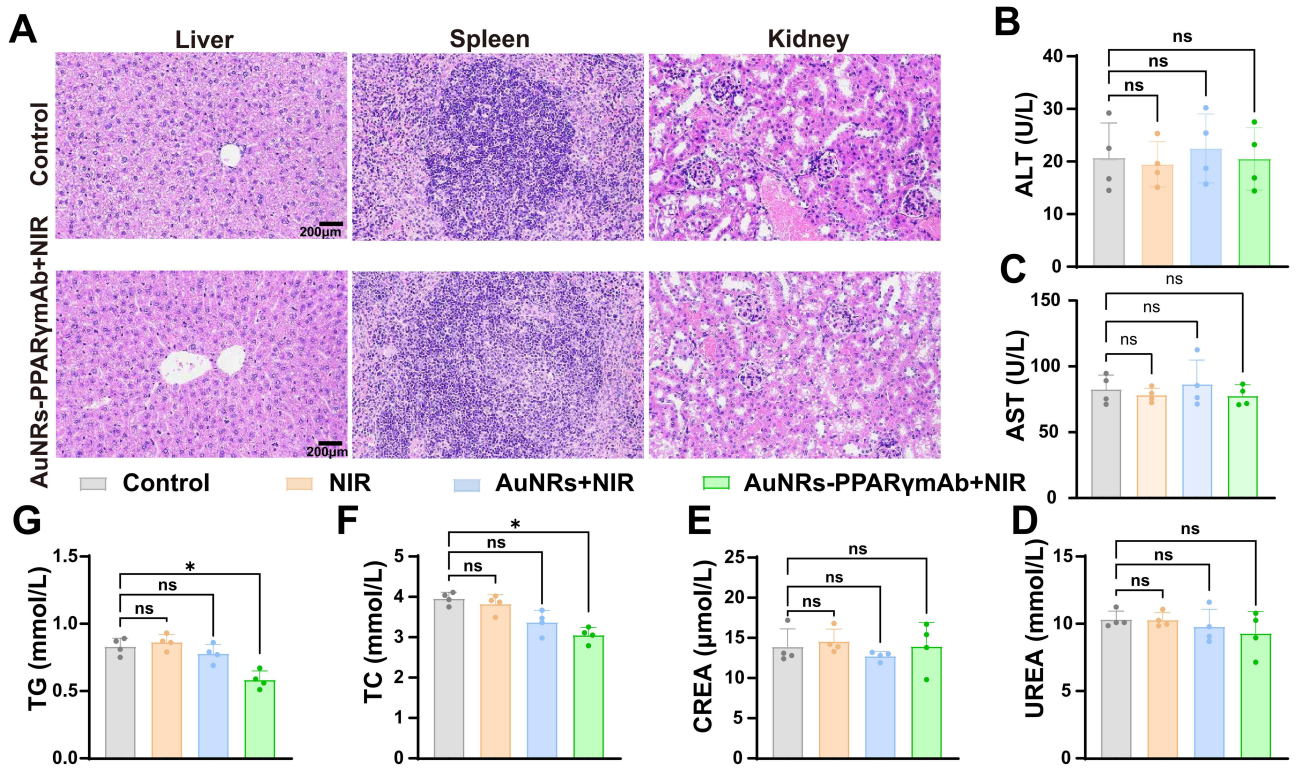


**Figure 7** In vivo Biocompatibility of AuNRs-PPARγmAb. (**A**) The HE staining of the liver, spleen, and kidneys in mice from the AuNRs+NIR and AuNRs-PPARγmAb+NIR groups. (**B**–**G**) Statistical analysis of liver enzymes (ALT, AST), lipid profiles (TG, TC), renal function (CREA), and urea levels in the Control, NIR, AuNRs+NIR, and AuNRs-PPARγmAb+NIR groups after 14 days. (ns, no significance, *P < 0.05).

## Discussion

For many years, having an aesthetically pleasing body shape has been a common goal for both men and women. Regardless of gender, many people desire to eliminate excess abdominal fat and sculpt their ideal body shape. Liposuction surgery is considered the gold standard for fat removal and body contouring, and it remains one of the most commonly performed surgeries.[25] In 2018, American plastic surgeons performed nearly 290,000 liposuction procedures, making it the second most common surgery after breast augmentation.[26] Compared to surgical treatments, non-surgical fat reduction techniques use methods such as medications, ultrasound, thermal damage, and lasers to disrupt fat cell membranes, thereby reducing local fat.[27] However, these methods often lack specificity, which can lead to damage to surrounding normal non-fat cells, triggering strong inflammatory responses and complications such as fibrosis and necrosis.[28–31] Therefore, developing safer and more effective non-surgical fat reduction methods is crucial.

Currently, AuNRs are considered excellent photothermal materials due to their ability to convert light energy into heat through the local surface plasmon resonance (LSPR) effect. Lowery et al were the first to inject gold nanocapsules into mice and achieve targeted tumor treatment through photothermal conversion under NIR laser irradiation. EI-Sayed et al chose near-infrared laser irradiation that matched the LSPR wavelength of gold nanorods, which induced photothermal conversion of nanoparticles in deep tissues, thereby killing cancer cells in deeper tissues.[32] Previous studies have mostly focused on using nanoparticles for photothermal therapy to target and kill tumor cells. In the field of non-tumor diseases, anti-CD31 gold nanorods (GNRs) nanoparticle platforms have been used for photothermal treatment of hemangiomas.[33] However, no studies have been reported in the field of fat reduction.

In our pursuit of a safer and more effective non-surgical fat reduction method, we propose an innovative approachusing laser-activated AuNRs-PPARγmAb to induce targeted apoptosis in fat cells. PPARγ is highly expressed in white adipose tissue and is an important transcriptional regulator of adipocyte development, widely present in various types of fat tissue.[34] This study investigates the effects of PPARγmAb conjugated to AuNRs, combined with NIR radiation, on fat cells. Previous studies have found that the extent of cell damage is closely related to the heat generated by AuNRs, with


https://doi.org/10.2147/IJN.S520656

the heat production depending on both the laser irradiation power and the intracellular uptake of AuNRs.[35,36] Our experimental results show that under the same NIR irradiation power, the AuNRs-PPARγmAb group significantly outperformed other groups in inhibiting fat cells. This result validates that AuNRs, after being conjugated with PPARγmAb, can specifically target fat cells, significantly increasing their uptake and retention time within the fat cells, thereby enhancing the local photothermal effect and substantially improving treatment efficacy.

Tumor hyperthermia involves using physical methods to heat tissue to 42–43.5°C and maintain it for 60–120 minutes to kill tumor cells.[37,38] The decrease in cell viability after AuNRs treatment may be caused by cell damage, death, or apoptosis. Our in vivo experiments indicate that AuNRs-PPARγmAb significantly reduce body weight in obese mice, and this weight loss is dependent on adipocyte apoptosis. Further analysis shows that in both in vitro and in vivo experiments, the apoptosis rate induced by AuNRs-PPARγmAb combined with NIR irradiation is significantly higher than that of the group using AuNRs alone, demonstrating stronger therapeutic effects. This significant difference is mainly attributed to the specific targeting ability of AuNRs-PPARγmAb.

By combining PPARγmAb with AuNRs, this study fully leverages the high expression of PPARγ in fat cells, successfully achieving precise targeting of fat cells. The main advantage of this targeted strategy is that it directly acts on fat cells without damaging surrounding normal tissues, effectively avoiding the common side effects seen in traditional treatments. Through this selective destruction mechanism, the treatment's safety is enhanced, and treatment efficiency is improved, providing both a theoretical foundation and practical evidence for the development of safer and more effective non-surgical fat reduction therapies.

Although the current results are encouraging, future research needs to address some key issues. First, the long-term stability and biodistribution of the AuNRs-PPARγmAb complex need further investigation to ensure its safety and effectiveness in clinical applications. Additionally, different administration routes and dosages need to be explored to optimize therapeutic effects and minimize potential side effects.

## Conclusion

In summary, our study successfully developed a novel non-surgical fat reduction method based on AuNRs conjugated with PPARγmAb. Experiments demonstrated that this complex can effectively induce adipocyte apoptosis and reduce localized fat tissue under NIR laser irradiation. The study showed that AuNRs-PPARγmAb complexes have high biocompatibility and targeting ability, capable of destroying adipocytes without harming surrounding tissues. In vivo results indicated that this method significantly reduces fat weight and thickness in obese mice with good safety profiles. Although promising, further research is needed to address the long-term stability and potential side effects of this method. Future studies will focus on optimizing conjugation techniques and laser parameters to enhance efficacy. This research provides a new approach to non-surgical fat reduction with significant clinical application potential.

## Data and Materials Availability

All data generated or analyzed during this study are included in this article, and further inquiries can be directed to Xiaojian Li.

## Ethics Approval and Consent to Participate

The use of clinical samples was approved by the Human Ethics Committee of Guangzhou Red Cross Hospital (Approval No. 2023-222-01). The animal experiments were approved by the Ethics Committee of Guangzhou Red Cross Hospital (Approval No. 2024-078-01) and were conducted in accordance with the Guide for the Care and Use of Laboratory Animals.

## Acknowledgments

The authors thank all individuals who participated in this work, as well as Microport Aesthmed Shanghai (Group) Co., Ltd, China, for providing the laser device.

## Author Contributions

All authors made a significant contribution to the work reported, whether that is in the conception, study design, execution, acquisition of data, analysis and interpretation, or in all these areas; took part in drafting, revising or critically reviewing the article; gave final approval of the version to be published; have agreed on the journal to which the article has been submitted; and agree to be accountable for all aspects of the work.

## Funding

This work is supported by the Guangzhou Health Science and Technology Guidance Program (20241A010015), the Guangzhou Clinical Key Specialty (Clinical Medical Research Institute) Construction Project, the Guangzhou Research-oriented Hospital (Major Difficult and Rare Diseases Diagnosis and Treatment Center) Construction Project, Basic and Applied Basic Research Foundation of Guangdong Province (2023A1515220237), and the Guangzhou Specialty Clinical Technology Project (2023C-TS46).

## Disclosure

The authors declare no potential conflicts of interest concerning this Article's research, authorship, and publication.

## References

1. Conway B, Rene A. Obesity as a disease: no lightweight matter. *Obesity Rev*. 2004;5(3):145–151. doi:10.1111/j.1467-789X.2004.00144.x
2. Müller TD, Blüher M, Tschöp MH, DiMarchi RD. Anti-obesity drug discovery: advances and challenges. *Nat Rev Drug Discov*. 2022;21(3):201–223. doi:10.1038/s41573-021-00337-8
3. Lotta LA, Wittemans LBL, Zuber V, et al. Association of genetic variants related to gluteofemoral vs abdominal fat distribution with type 2 diabetes, coronary disease, and cardiovascular risk factors. *JAMA*. 2018;320(24):2553–2563. doi:10.1001/jama.2018.19329
4. Piché ME, Tchernof A, Després JP. Obesity phenotypes, diabetes, and cardiovascular diseases. *Circ Res*. 2020;126(11):1477–1500. doi:10.1161/CIRCRESAHA.120.316101
5. Perdomo CM, Cohen RV, Sumithran P, Clément K, Frühbeck G. Contemporary medical, device, and surgical therapies for obesity in adults. *Lancet*. 2023;401(10382):1116–1130. doi:10.1016/S0140-6736(22)02403-5
6. Seretis K, Goulis DG, Koliakos G, Demiri E. Short- and long-term effects of abdominal lipectomy on weight and fat mass in females: a systematic review. *Obes Surg*. 2015;25(10):1950–1958. doi:10.1007/s11695-015-1797-1
7. Jewell ML, Solish NJ, Desilets CS. Noninvasive body sculpting technologies with an emphasis on high-intensity focused ultrasound. *Aesthetic Plast Surg*. 2011;35(5):901–912. doi:10.1007/s00266-011-9700-5
8. Wu S, Coombs DM, Gurunian R. Liposuction: concepts, safety, and techniques in body-contouring surgery. *Cleve Clin J Med*. 2020;87(6):367–375. doi:10.3949/ccjm.87a.19097
9. Beidas OE, Gusenoff JA. Update on liposuction: what all plastic surgeons should know. *Plast Reconstr Surg*. 2021;147(4):658e–668e. doi:10.1097/PRS.0000000000007419
10. Matarasso A, Matarasso DM, Matarasso EJ. Abdominoplasty: classic principles and technique. *Clin Plast Surg*. 2014;41(4):655–672. doi:10.1016/j.cps.2014.07.005
11. Pollock T, Pollock H. Progressive tension sutures in abdominoplasty. *Clin Plast Surg*. 2004;31(4):583–589, vi. doi:10.1016/j.cps.2004.03.015
12. Jabbour S, Awaida C, Mhawej R, Bassilios Habre S, Nasr M. Does the addition of progressive tension sutures to drains reduce seroma incidence after abdominoplasty? A systematic review and meta-analysis. *Aesthet Surg J*. 2017;37(4):440–447. doi:10.1093/asj/sjw130
13. Klein SM, Schreml S, Nerlich M, Prantl L. In vitro studies investigating the effect of subcutaneous phosphatidylcholine injections in the 3T3-L1 adipocyte model: lipolysis or lipid dissolution? *Plast Reconstr Surg*. 2009;124(2):419–427. doi:10.1097/PRS.0b013e3181adce61
14. Pereira JX, Cavalcante Y, Wanzeler de Oliveira R. The role of inflammation in adipocytolytic nonsurgical esthetic procedures for body contouring. *Clin Cosmet Invest Dermatol*. 2017;10:57–66. doi:10.2147/CCID.S125580
15. Mulholland RS, Paul MD, Chalfoun C. Noninvasive body contouring with radiofrequency, ultrasound, cryolipolysis, and low-level laser therapy. *Clin Plast Surg*. 2011;38(3):503–520, vii–iii. doi:10.1016/j.cps.2011.05.002
16. Zhang Y, Yu J, Qiang L, Gu Z. Nanomedicine for obesity treatment. *Sci China Life Sci*. 2018;61(4):373–379. doi:10.1007/s11427-017-9257-1
17. Sibuyi NRS, Moabelo KL, Meyer M, Onani MO, Dube A, Madiehe AM. Nanotechnology advances towards development of targeted-treatment for obesity. *J Nanobiotechnol*. 2019;17(1):122. doi:10.1186/s12951-019-0554-3
18. Xiao Q, Tang L, Chen S, et al. Two-pronged attack: dual activation of fat reduction using near-infrared-responsive nanosandwich for targeted anti-obesity treatment. *Adv Sci*. 2024;11(43):e2406985. doi:10.1002/advs.202406985
19. Su Y, Wang W, Xiao Q, et al. Macrophage membrane-camouflaged lipoprotein nanoparticles for effective obesity treatment based on a sustainable self-reinforcement strategy. *Acta Biomater*. 2022;152:519–531. doi:10.1016/j.actbio.2022.08.055
20. Choi H, Hong J, Seo Y, et al. Self-assembled oligopeptoplex-loaded dissolving microneedles for adipocyte-targeted anti-obesity gene therapy. *Adv Mater*. 2024;36(16):e2309920. doi:10.1002/adma.202309920
21. Sobolev VV, Tchepourina E, Korsunskaya IM, et al. The role of transcription factor PPAR-γ in the pathogenesis of psoriasis, skin cells, and immune cells. *Int J Mol Sci*. 2022;23(17):9708. doi:10.3390/ijms23179708
22. García-Alonso V, López-Vicario C, Titos E, et al. Coordinate functional regulation between microsomal prostaglandin E synthase-1 (mPGES-1) and peroxisome proliferator-activated receptor γ (PPARγ) in the conversion of white-to-brown adipocytes. *J Biol Chem*. 2013;288(39):28230–28242. doi:10.1074/jbc.M113.468603

23. Lefterova MI, Haakonsson AK, Lazar MA, Mandrup S. PPARγ and the global map of adipogenesis and beyond. *Trends Endocrinol Metab*. 2014;25(6):293–302. doi:10.1016/j.tem.2014.04.001
24. Overchuk M, Weersink RA, Wilson BC, Zheng G. Photodynamic and Photothermal Therapies: synergy Opportunities for Nanomedicine. *ACS Nano*. 2023;17(9):7979–8003. doi:10.1021/acsnano.3c00891
25. Matarasso A, Swift RW, Rankin M. Abdominoplasty and abdominal contour surgery: a national plastic surgery survey. *Plast Reconstr Surg*. 2006;117(6):1797–1808. doi:10.1097/01.prs.0000209918.55752.f3
26. American Society for Aesthetic Plastic Surgery. The American Society for Aesthetic Plastic Surgery's Cosmetic Surgery National Data Bank: statistics 2018. *Aesthet Surg J*. 2019;39(Suppl_4):1–27. doi:10.1093/asj/sjz164
27. Kennedy J, Verne S, Griffith R, Falto-Aizpurua L, Nouri K. Non-invasive subcutaneous fat reduction: a review. *J Eur Acad Dermatol Venereol*. 2015;29(9):1679–1688. doi:10.1111/jdv.12994
28. Mendez BM, Coleman JE, Kenkel JM. Optimizing patient outcomes and safety with liposuction. *Aesthet Surg J*. 2019;39(1):66–82. doi:10.1093/asj/sjy151
29. Illouz YG. Complications of liposuction. *Clin Plast Surg*. 2006;33(1):129–163, viii. doi:10.1016/j.cps.2005.10.001
30. Fagien S, McChesney P, Subramanian M, Jones DH. Prevention and management of injection-related adverse effects in facial aesthetics: considerations for ATX-101 (Deoxycholic Acid Injection) treatment. *Dermatologic Surg*. 2016;42(Suppl 1):S300–s304. doi:10.1097/DSS.0000000000000898
31. Deligonul FZ, Yousefian F, Gold MH. Literature review of adverse events associated with cryolipolysis. *J Cosmet Dermatol*. 2023;22(Suppl 3):31–36. doi:10.1111/jocd.16000
32. Huang X, El-Sayed IH, Qian W, El-Sayed MA. Cancer cells assemble and align gold nanorods conjugated to antibodies to produce highly enhanced, sharp, and polarized surface Raman spectra: a potential cancer diagnostic marker. *Nano Lett*. 2007;7(6):1591–1597. doi:10.1021/nl070472c
33. Jiang Y, Liu J, Qin J, et al. Light-activated gold nanorods for effective therapy of venous malformation. *Mater Today Bio*. 2022;16:100401. doi:10.1016/j.mtbio.2022.100401
34. Mota de Sá P, Richard AJ, Hang H, Stephens JM. Transcriptional Regulation of Adipogenesis. *Compr Physiol*. 2017;7(2):635–674. doi:10.1002/j.2040-4603.2017.tb00753.x
35. Zhou R, Zhang M, Xi J, et al. Gold nanorods-based photothermal therapy: interactions between biostructure, nanomaterial, and near-infrared irradiation. *Nanoscale Res Lett*. 2022;17(1):68. doi:10.1186/s11671-022-03706-3
36. Nejabat M, Samie A, Ramezani M, Alibolandi M, Abnous K, Taghdisi SM. An overview on gold nanorods as versatile nanoparticles in cancer therapy. *J Control Release*. 2023;354:221–242. doi:10.1016/j.jconrel.2023.01.009
37. Zhu W, Pan S, Zhang J, et al. The role of hyperthermia in the treatment of tumor. *Crit Rev Oncol Hematol*. 2024;204:104541. doi:10.1016/j.critrevonc.2024.104541
38. Wang J, Wu X, Shen P, et al. Applications of inorganic nanomaterials in photothermal therapy based on combinational cancer treatment. *Int J Nanomed*. 2020;15:1903–1914. doi:10.2147/IJN.S239751